WILLIAM JOEL DIETMAR JOHNSON

*Candidate*

ELECTRICAL AND COMPUTER ENGINEERING

*Department*

This thesis is approved, and it is acceptable in quality and form for publication on microfilm:

*Approved by the Thesis Committee:*

Peter Dorato, Chairperson

Chaouki Abdallah

Fred Luthan

Accepted: E Uhlenkamp

Asst. *Dean, Graduate School*

April 23, 1990

*Date*

# ROBUST CONTROL OF RF POWER SYSTEMS FOR PARTICLE ACCELERATORS

BY

WILLIAM JOEL DIETMAR JOHNSON

B.S., Auburn University, 1983

THESIS

Submitted in Partial Fulfillment of the
Requirements for the Degree of

Master of Science in Electrical Engineering

The University of New Mexico
Albuquerque, New Mexico

MAY 1990

**ACKNOWLEDGEMENTS**

No research is conducted without the mutual benefit of interaction among many people. Although the list of collaborators would be too long to list, I would, nevertheless, like to acknowledge several particularly helpful individuals. First are my parents for instilling in me the attitude of the benefit of a good education. Next is Dr. Richard Sheffield, my group leader, for believing in my research and graduate studies and encouraging me to complete both. My thesis advisor, Dr. Chaouki Abdallah, provided continued and helpful support throughout my graduate control studies and research, thank you. My thanks to Dr. Peter Dorato and Dr. Bruce Carlsten for agreeing to be on my advisory committee. Also, my thanks to the gang at the Los Alamos FEL facility for allowing me the time necessary to conduct my experiments. A hearty thank you to Noel Okay, for excellent technician support, and David Baca, for drawing all the figures in my thesis. Last, but definitely not least, my thanks to the gals at Secretarial Office Services, without whose typing of this manuscript I surely would not have met the thesis deadline.

# ROBUST CONTROL OF RF POWER SYSTEMS FOR PARTICLE ACCELERATORS

BY

WILLIAM JOEL DIETMAR JOHNSON

ABSTRACT OF THESIS

Submitted in Partial Fulfillment of the
Requirements for the Degree of

**Master of Science in Electrical Engineering**

The University of New Mexico
Albuquerque, New Mexico

MAY 1990

**Robust Control of rf Power Systems**

**For Particle Accelerators**

William Joel Dietmar Johnson

B.S. Electrical Engineering, Auburn University, 1983

M.S. Electrical Engineering, University of New Mexico, 1990

In this thesis we discuss a novel technique for controlling the phase and the amplitude of the electric fields in an accelerator. The new controller's advantages are greater loop gain, ease of implementation, greater stability robustness, less controller cost, and greatly simplified hardware.

The designed controller is an optimal linear quadratic regulator (LQR) state-feedback. We contrast it with the previously used output-feedback scheme. The limitations of the output-feedback technique are discussed and shown not to exist for the LQR controller. Finally, the experimental results are presented and directions for future research are described.

## TABLE OF CONTENTS

# INTRODUCTION

One application of an electron particle accelerator is to drive a Free-Electron Laser (FEL). The FEL generates coherent radiation by passing an electron beam through an alternating magnetic field, called an undulator, which produces coherent photons whose wavelength is proportional to the incident electron beam energy. The FEL performance critically depends on the properties of the incident electron beam. The equation of resonance for FELs is given approximately by

$$\lambda_L \approx \frac{\lambda_\omega}{2\gamma^2} \quad , \tag{1}$$

where $\lambda_L$ is the laser wavelength, $\lambda_\omega$ is the undulator magnetic field period, and $\gamma$ is the relativistic mass factor of the incident electron beam. In order for the FEL to operate efficiently, theory projects that the fluctuations in $\gamma$ must be less than the small-signal gain bandwidth, which is proportional to $1/(2N)$, where N is the number of periods in the undulator. At Los Alamos National Laboratory there is an FEL experiment presently operating. The present number of periods in the undulator is 40. In addition, experiments have shown that to generate radiation of a constant-intensity and wavelength, the energy fluctuations must be much less than $1/(2N)$ [1]. Our goal is to minimize the variations of $\gamma$, in

order to give efficient, constant-intensity, single-wavelength radiation. Fluctuations in $\gamma$ <0.2% has been chosen as our design goal. The factors that give rise to energy fluctuations in the electron beam are the variations in the accelerating electric fields and in the electron injector. This thesis focuses only on controlling the variations in the electric fields. The consequences of fluctuations produced by the electron injector will be ignored. The electric fields have both phase and amplitude components whose variations contribute to the energy fluctuations, which in turn, directly produce variations in $\gamma$.

Previously, the control configuration was an output feedback with lead-lag compensation. The electric field feedback signal from the accelerator was first resolved into its phase and amplitude components, each having its own control loop (Fig. 1). However, because the two loops are coupled, their separation can never be complete, nor is it necessary. Since the system that produces the electric fields contains nonlinearities and many uncertain parameters, the previous control system must be frequently tuned when operating conditions are changed. In addition, because of the simple structure of the compensator, the resulting performance is limited.

In this thesis, we present a realistic model of the accelerator system that reduces the number of internal states to 3 as well as reducing the size of the uncertainties. The

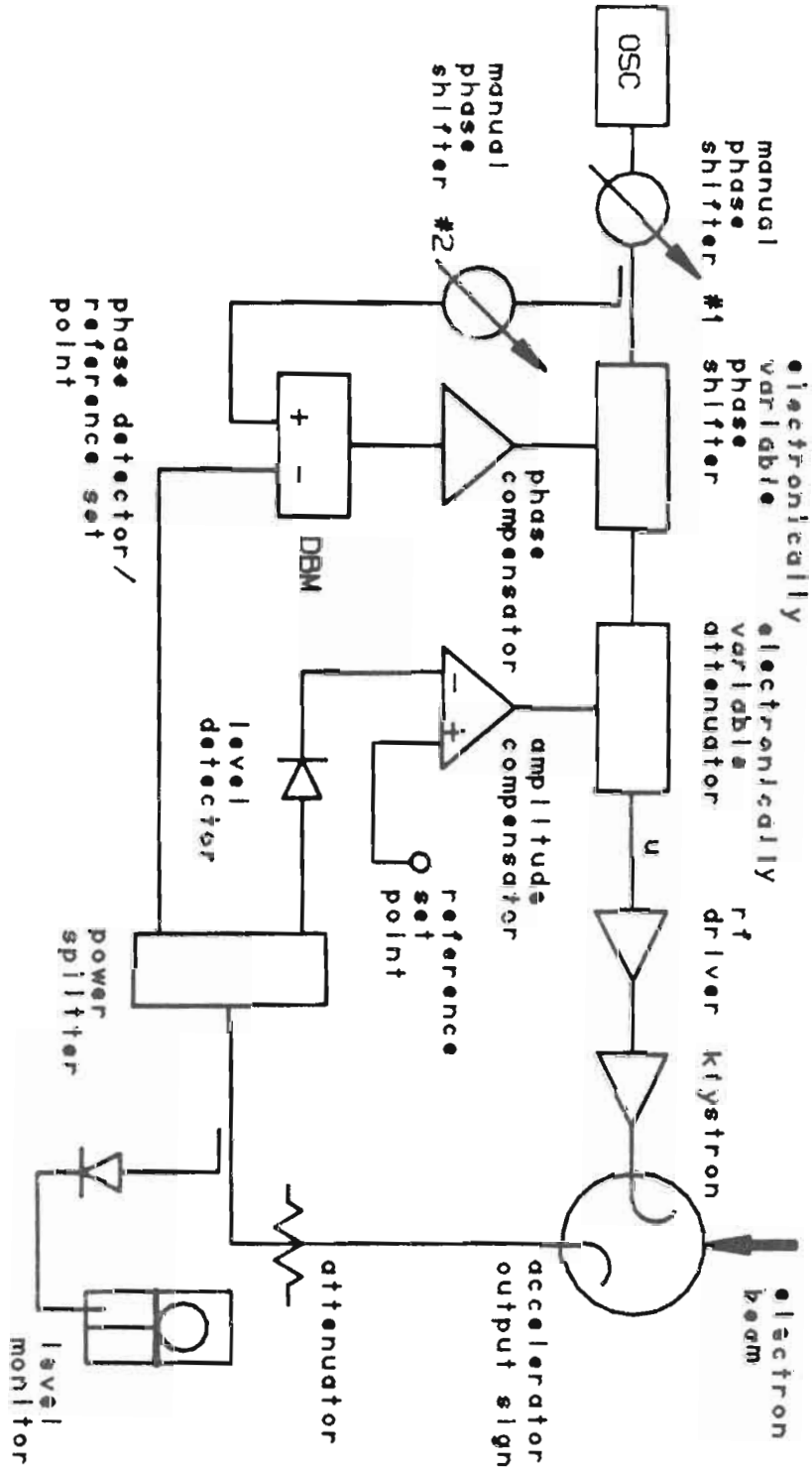


FIGURE 1 Old LANL Output Feedback Scheme.

model shown in Fig. 2 is expressed to a first approximation by the linear state equation

$$dx/dt = Ax + bu \tag{2}$$

$$y = Cx \tag{3}$$

where A and b contain the system's parameters, x(t) is the state vector, and u is the scalar input. In this model, some of the entries of the A and b matrices are uncertain. However, bounds on these entries are known.

The designed controller is an optimal Linear quadratic regulator (LQR) state-feedback as opposed to the output-feedback used before. There are four major advantages of this new approach. The first is the significant reduction in energy fluctuation over the old control system. The second is the improved stability robustness over the previous technique. The third is the greatly simplified hardware. The fourth is that the feedback gains are implemented using only passive elements. This thesis will report on both the analytic design and hardware implementation of the new robust control system.

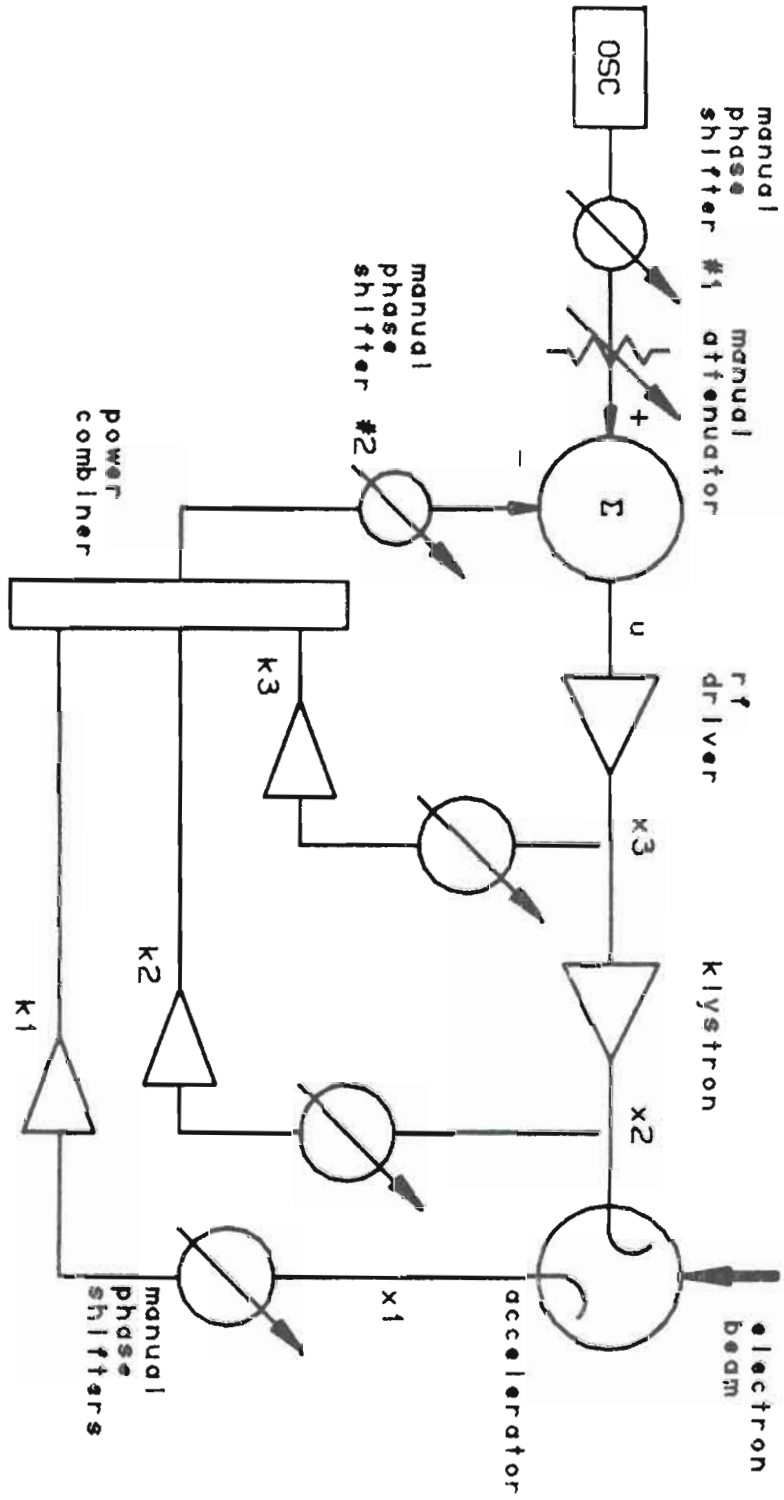


FIGURE 2 State Feedback Controller.

# CHAPTER I. THEORY

## A. Accelerator Theory

The electron linear accelerator was a direct outcome of the knowledge gained during World War II about waveguides. The electron linear accelerator (linac) derives its name from the fact that the flight pattern of an electron, from beginning to end, is a straight line. We now introduce our first fact [2].

> Fact 1: An electron (or ensemble of electrons) of charge q (or net charge q) moving along a distance L in an uniform electric field $\mathscr{E}$ will acquire an energy,

$$E = q\mathscr{E}L \tag{4}$$

In order to accelerate an electron to a given energy, one can either use a weak field and let the particle travel a long distance, or a strong field and let the particle travel a short distance.

There are two important concepts regarding waveguides that need to be understood, i.e., phase velocity and group velocity. The velocity of propagation of a wavefront along a wave guide is less than its velocity in free space. The slower wavefront velocity is due to the way the

electromagnetic field travels. Electromagnetic waves zigzag back and forth across the guide at the velocity of light. But due to the length of path, the wavefront (or head) of the zigzag actually travels slower along the guide (Fig. 3).

Definition 1: The axial velocity of an electromagnetic wavefront or a group of waves is called the group velocity, denoted $V_G$.

The relationship between the group velocity and its diagonal component produces a strange phenomenon. The velocity of propagation is greater than the speed of light. A wavefront (head of zigzag) will move along a diagonal path from one point to another point a distance L at the velocity of light $V_L$. Due to this diagonal movement, during this time the wavefront has actually moved axially down the guide a distance G at a group velocity $V_G$. However, along the wall of the guide, the phase of the wave has moved a distance P, a distance greater than L or G (Fig. 4).

Definition 2: The axial velocity of the phase of an electromagnetic wave is called the phase velocity, denoted $V_P$.

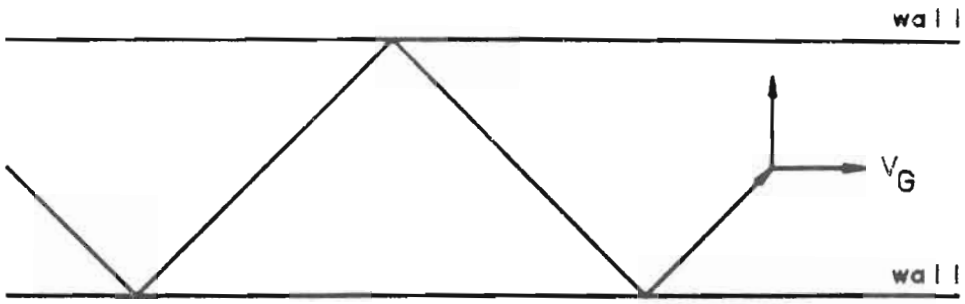


FIGURE 3 Waveguide Group Velocity.

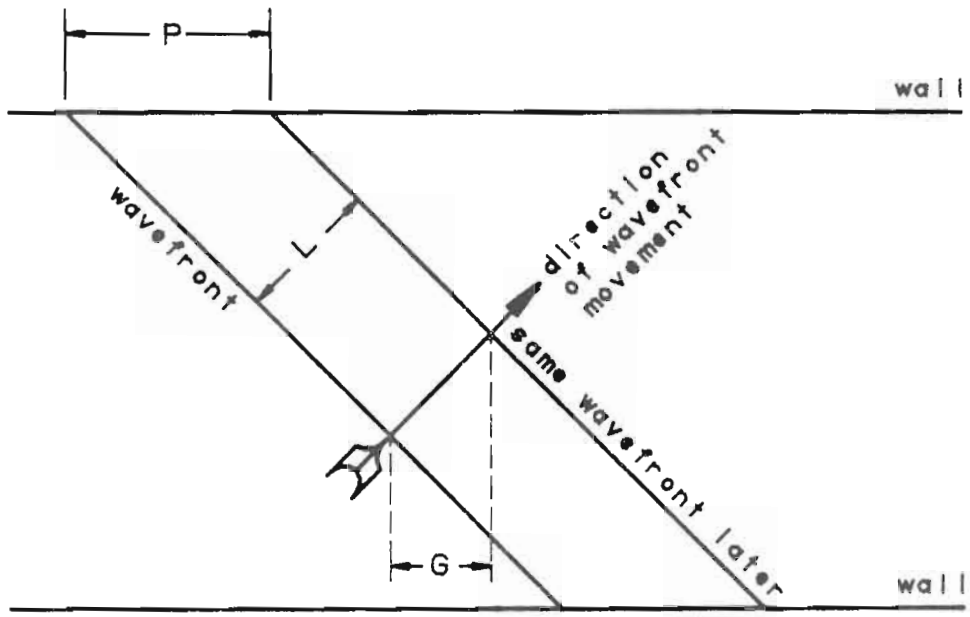


FIGURE 4 Waveguide Phase Velocity.

A mathematical relationship between the three velocities is given by the equation

$$V_L=\sqrt{V_P V_G} \quad , \tag{5}$$

where $V_L$ = velocity of light

$V_P$ = phase velocity

$V_G$ = group velocity.

It is instructive to draw an analogy between the waveguide's phase velocity and an ocean shoreline. Let observers be placed at arbitrary intervals along the beach shoreline. Further, suppose that an incoming wave has a direction of propagation that is at an angle with respect to the beach. Then, these same observers will see the crest pass by each of them, say right to left, in a very short time. Whereas, the incoming propagation speed of the wavehead, say from some point out to sea, is possibly only a few feet per second. The propagation of the crest along the shoreline is the phase velocity. If the direction of propagation were perpendicular to the shoreline, then the phase velocity would be infinite, i.e., all observers would see the crest strike the shore at the same time. Conversely, if the direction of the wave were parallel to the shore, then the observers would see the crest pass by each of them at a speed given by the wave velocity.

Returning to waveguides, the practical effect of the above is that if the microwave frequency being propagated is modulated, the modulation envelope will move forward at the group velocity, while the individual cycles of microwave energy will propagate through the modulation envelope at the phase velocity.

In general, information is conveyed by modulating a carrier signal. Therefore, the information of a modulated wave traveling through a waveguide propagates at the group velocity. We now have our second important fact.

> Fact 2: The control of a microwave carrier in an accelerator is governed by the group velocity of the structure.

Unfortunately, smooth-walled waveguides could never be used to accelerate electrons. This is because $V_p$ is greater than the speed of light, $V_l$. Thus, the phase velocity always exceeds that which any particle can attain, regardless of its energy, and the waves will pass the particle alternately accelerating and decelerating it.

A practical method of slowing the phase velocity is to introduce some inductance into the walls of the cylindrical waveguide. If the inner surface of the guide is sharply corrugated with disks so that the original guide diameter, 2b, now has a center hole with diameter 2a, and if the radial

difference, b-a, is less than a quarter wavelength of the accelerating electric field wavelength, then inductance will be added to the circuit; hence, $V_p$ will be lowered (Fig. 5). Consequently, an electron could be indefinitely accelerated if the wave's phase velocity could be adjusted to maintain synchronism with the particle's velocity.

The value of "b" is set by the wavelength at which the designer wishes to operate the accelerator or by the available high power microwave (more commonly referred to as radio-frequency, rf) sources. The distance between disk sides or the distance between the center of adjacent cells is determined by which mode the accelerator is to be operated in. The mode of a structure is the amount of phase shift that exists from one cell to an adjacent cell.

There are two types of accelerators used to give electrons energy, the traveling wave (TW) or the standing wave (SW) accelerator. Both accelerators have their obvious name interpretations. At the Los Alamos National Laboratory (LANL) Free-electron Laser (FEL) facility the standing wave accelerator is used. In order to couple power from one cell to another cell, the so-called side-coupled linac was developed during the early sixties at Los Alamos [3]. Electrically, this structure is a $\pi/2$-mode accelerator, but in terms of its interaction with the electron beam it is a $\pi$-mode unit. As shown in Fig. 5, the side-coupled linac derives its name from the position of the coupling cells with respect to

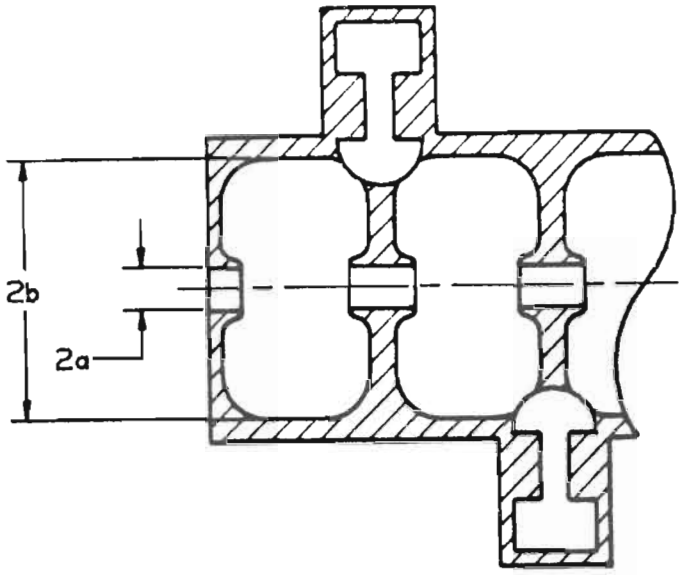


a) side coupled linac

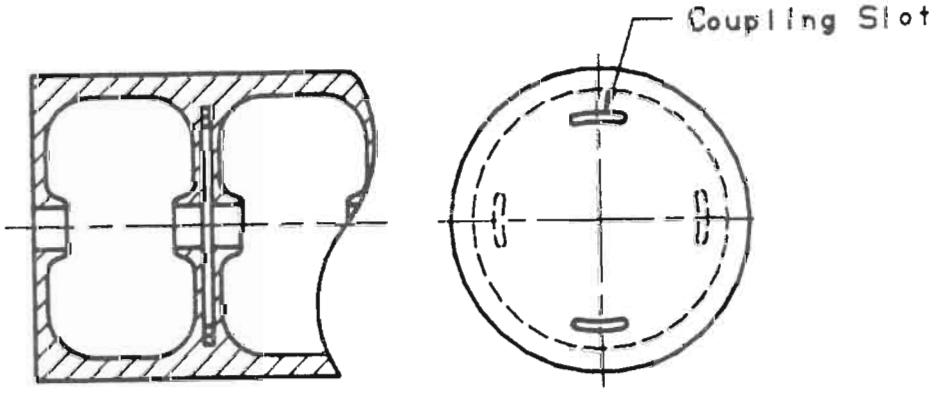


b) on-axis coupled linac

FIGURE 5 Two Versions of a $\frac{\Pi}{2}$-mode Accelerator.

the accelerating cells. In addition, the FEL facility utilizes an on-axis coupled structure (Fig. 5). This accelerator is also a standing wave, $\pi/2$-mode structure.

The advantage of $\pi/2$-mode accelerators is that their group velocity is at its greatest value relative to other mode structures, permitting both good interaction between electric field and electron beam and also good control of the electric field. The advantage of $\pi$-mode accelerators is that their field distribution patterns are uniform from one cell to the next, virtually identical to one another. Therefore, SW accelerators have two good properties: high group velocity and identical field gradients from cell-to-cell. This in turn gives our third fact.

Fact 3: A sufficient description of standing wave accelerators is their total Input-to-Output properties.

An additional design requirement for accelerators is their individual cavity field distribution patterns.

The $TM_{01}$-mode is the ideal field pattern for particle acceleration. This is because the peak-on-axis electric field is precisely where the electrons interact and gain energy (Fig. 6).

To calculate the required rf power to achieve a given energy, one proceeds in the following manner:

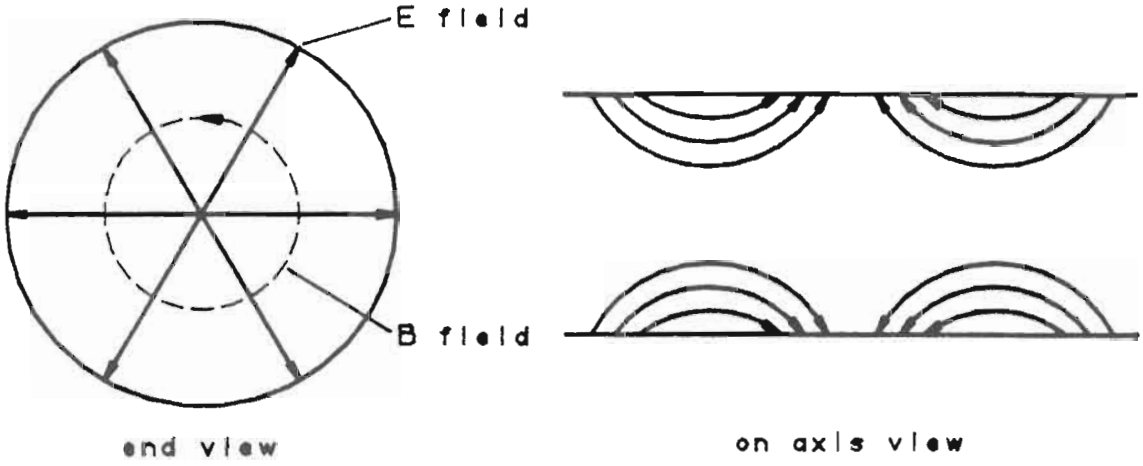


a) cylindrical waveguide

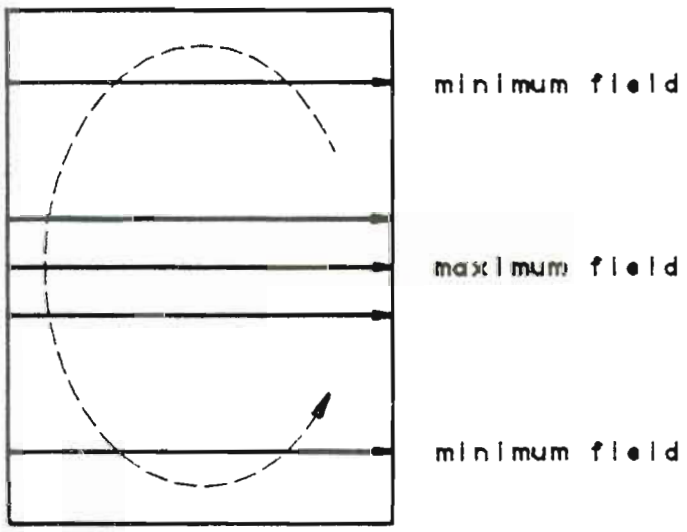


b) cylindrical cavity

FIGURE 6 $TM_{01}$ Mode.

$$R_o = \frac{(\int_0^{\ell} E_z \, dz)^2}{P_{total}} \quad , \tag{6}$$

where $R_o$ = the shunt impedance

$E_z$ = the peak on-axis electric field

$P_{total}$ = the total power dissipated in the structure.

Therefore, the structure power is given by

$$P_s = \frac{V^2}{R_o L} \quad , \tag{7}$$

where $P_s$ = the structure power

V = the total desired voltage gain of the particle

$R_o$ = the shunt impedance per meter

L = the total length of accelerator

and the beam power is given by

$$P_b = VI_b \quad , \tag{8}$$

where V = the beam voltage

$I_b$ = the average beam current.

The total power is $P_t = P_s + P_b + P_c$, where $P_c$ is the added power reserve needed for electric field control.

There are many more issues that could be discussed related to accelerator theory; however, this is beyond the scope of this thesis. This introduction is meant only to convey the minimum amount of information necessary to comprehend the basics of acceleration. For more detailed information, the author refers the interested reader to any one of a number of particle accelerator journals or books [2,4].

## B. Free-electron Laser Theory

Basically, a Free-electron Laser (FEL) is a classical, i.e., nonquantum mechanical, device that converts the kinetic energy of unbounded electrons, spatially and temporally grouped together, to electromagnetic radiation. The FEL is a coherent, tunable source of radiation. This conversion process occurs when a relativistic electron beam passes through a transverse, periodic, magnetic field, called an undulator (Fig. 7). The device is classical in the sense that the methods of quantum mechanics are unnecessary. A conventional laser works on the principle of inverting electrons from their ground states and is capable of amplifying incoming radiation at wavelengths near or equal to that of the atomic transition [5].

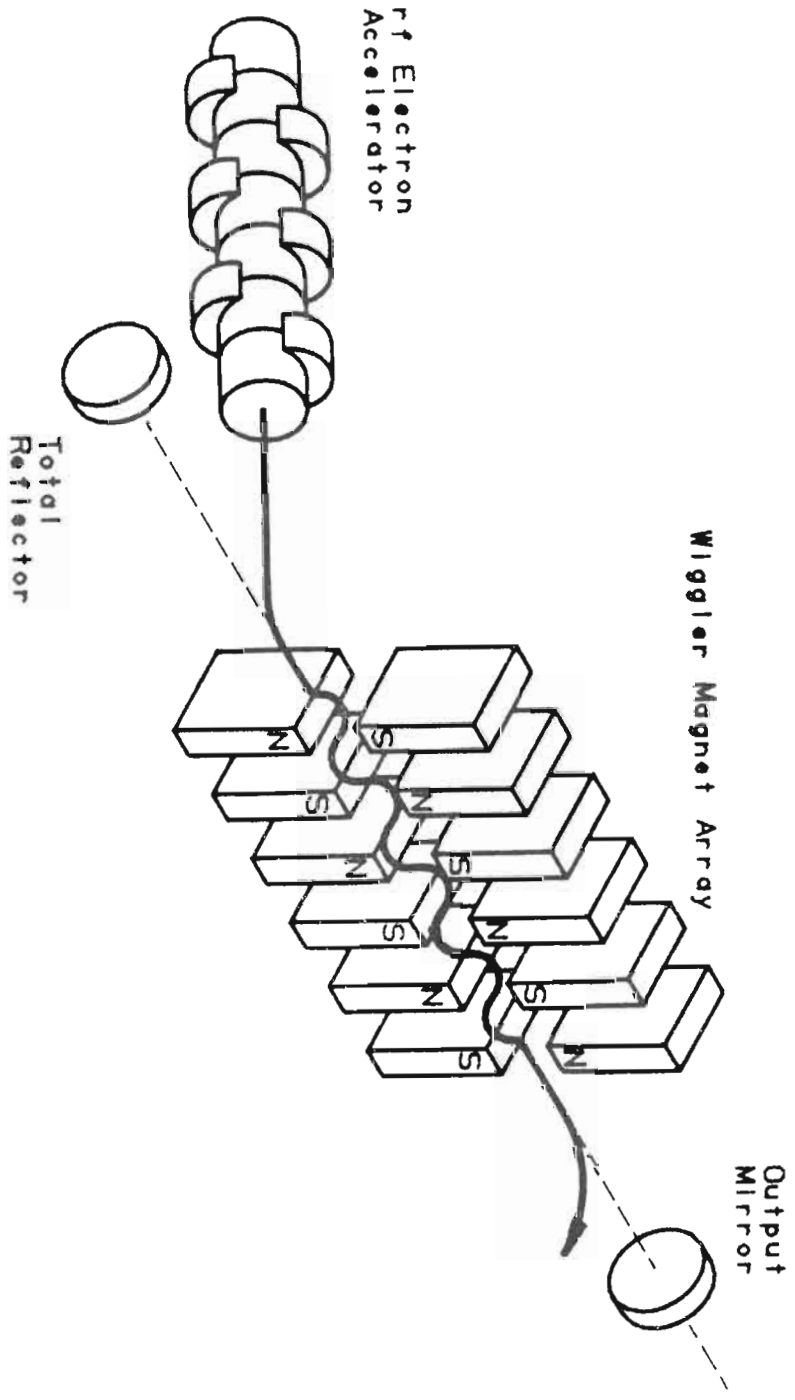


FIGURE 7 Accelerator and FEL Schematic.

The fundamental equation for FELs is the condition of resonance, which is given by

$$\lambda_L = \frac{\lambda_\omega}{2\gamma^2}\,(1+K^2) \quad , \tag{9}$$

where $\lambda_L$ is the FEL output wavelength, $\lambda_\omega$ is the period of the undulator, $\gamma$ is the ratio of the electron's kinetic energy to its rest energy, and K is a measure of the peak magnetic field in the undulator.

The radiation wavelength can be easily tuned simply by varying the electron beam energy. Since electrons have a small mass they become relativistic at very low energies. At 2 MeV the electrons have a velocity approximately ninety-seven percent of the speed of light [2]. Our accelerator has an approximate on on-axis accelerating gradient of 8 MeV/m; therefore, in just a few cells the beam is fully relativistic, and all cells are equally spaced. In order to tune the laser wavelength then, all that is necessary is to change the input rf power; the particles will stay in synchronism with the accelerating phase and the output frequency of the laser will commensurately change. Therefore, in order to have constant wavelength radiation, the electron beam energy must be kept constant.

How constant the energy must be kept can be determined from the properties of the undulator's interaction with the

electron beam. The gain curve of a FEL is antisymmetric [6]. Half of the curve is positive and half is negative. The width of the positive half is proportional to 1/(2N), where N is the total number of periods in the undulator. Therefore, in order to have constant-intensity, constant-wavelength radiation, the variations in electron beam energy must be less than 1/(2N).

Because of the nature of the accelerator, not every rf cycle is used to trap and accelerate electrons. Filling every rf cycle would result in a very high average current. From P = VI, this case of high average current would require a greater total rf power than is necessary. Therefore, only one cycle out of many cycles is used. At Los Alamos FEL facility, one out-of-every 60 rf cycles accelerates electrons.

The output of the laser will have the same timing structure as the electron beam. But since photons travel at the speed of light and electrons slightly slower, the phase of the rf power must also be controlled. The electrons and the photons overlap and interact with one another inside the undulator. The extent to which this interaction occurs is governed by the timing jitter of the arriving electrons, which in turn is produced by the phase fluctuations of the accelerating electric field. Acceptable levels of phase variation is determined by the pulse width of the ensemble of electrons, called a micropulse (Fig. 8). Micropulses should not have a timing jitter greater than ten percent of their pulse width. The corresponding phase requirement can be

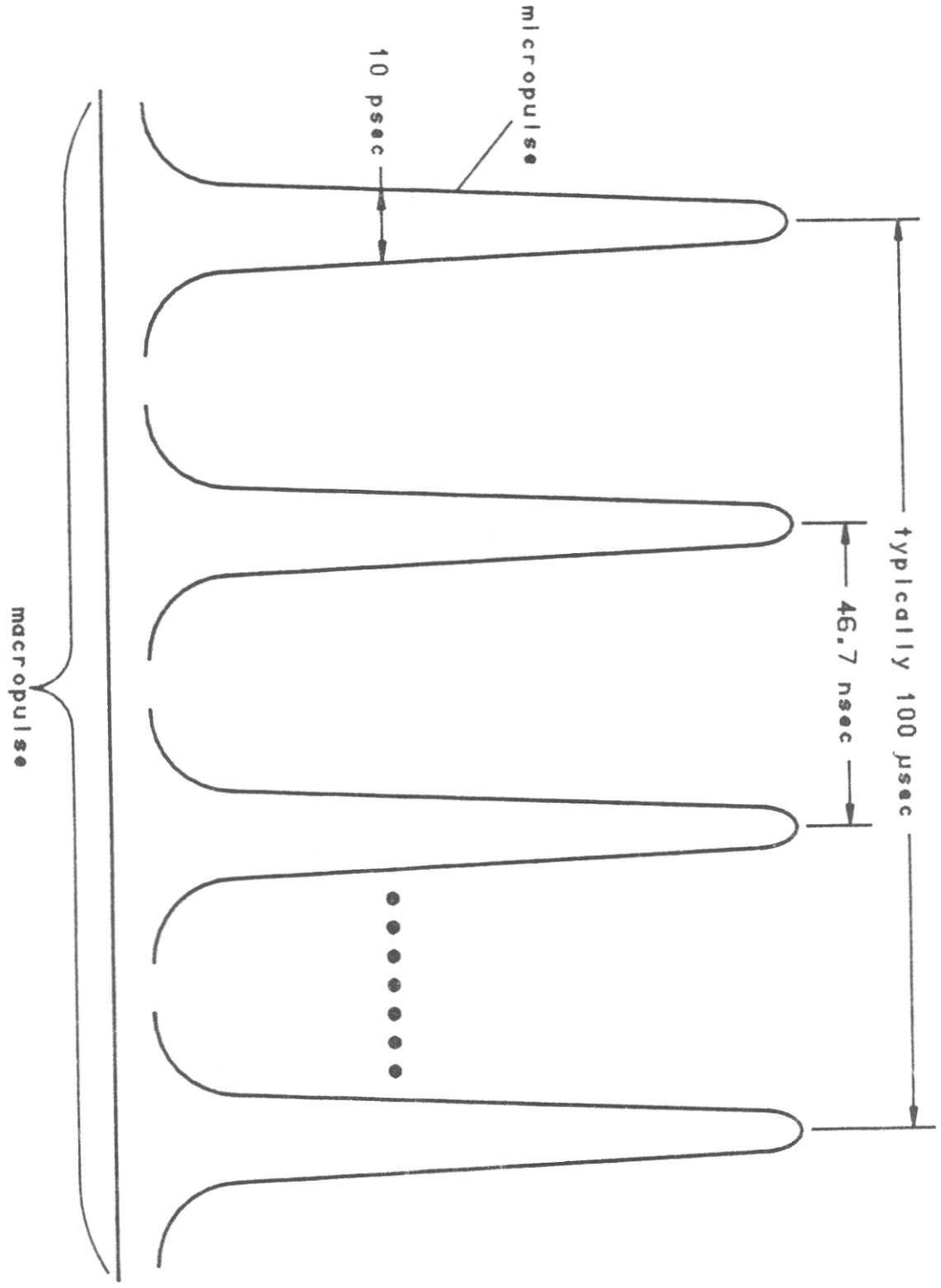


FIGURE 8 Micropulse and Macropulse.

calculated by multiplying the time jitter requirement by 360°, and then multiplying that result by the rf accelerating frequency.

With the phase and amplitude fluctuations under control, each successive electron micropulse will give up some of its energy, through an acceleration process, in the form of a photon of radiation. Each of these new photons will add coherently to the photon micropulse already present. This process continues until radiation intensity saturation is achieved. Saturation is achieved when the electrons lose approximately 1/(2N) percent of their energy. A photon is produced because radiation occurs whenever an energetic electron is subject to an accelerating force. In the undulator the magnetic field changes the direction of travel of the electron, which results in the electron radiating some of its energy in the form of a photon.

The subject of FELs is vast and extensive, but a thorough treatment is not possible in this manuscript [6]. The ideas presented in this chapter are necessary in order to understand the statement of the control problem given in the next chapter.

## CHAPTER II. STATEMENT OF CONTROL PROBLEM

Since in one out of every sixty rf cycles, an electron bunch enters, perturbs, and removes energy from the accelerating electric field, the rf control system is limited in its ability to correct these induced field errors. It is limited for three reasons: 1) the rf power frequency is 1300 Mhz; therefore, the electron perturbation frequency is one sixtieth of 1300 Mhz, or 21.67 Mhz, 2) the group velocity for a TW is given by $V_g = P/W$, where P is the rf power flow and W is the stored energy per unit length of the TW restoring the electric fields, and 3) there are practical limits on available peak power rf sources. The rf peak power available at the FEL facility is 6.5 MW and the open-loop bandwidth of the accelerator is 167 Khz. The quiescent operating rf power, due to electron beam and structure power requirements, is 4 MW. Because the perturbation frequency is 21.67 Mhz, the accelerator bandwidth is 167 Khz, and the rf surplus peak power is limited; the rf control system can never correct the high frequency-induced field errors. The same argument can be made for correcting the electron micropulse timing errors that are also due to problems in the injector.

Fact 5: The frequency response of field errors induced by the electron injector into the accelerator can be corrected if, and only if, the rf control system

bandwidth encompasses the induced field error bandwidth.

Given Fact 5, the electron injector must be controlled. Controlling the injector will be the only method to reduce to as near zero as possible any residual field errors not corrected by the rf control system.

The number of periods in the Los Alamos undulator is 40. The micropulse pulse width is 10 psec. Therefore, amplitude fluctuations less than 1.25% and phase variations less than 0.47° are necessary, but not sufficient. Experiments have shown that more stringent requirements are necessary [1]. Therefore, the control objectives are stated as follows:

1) The rf power shall be regulated in such a manner that the residual field amplitude error shall be less than or equal to 0.2%.
2) The rf power shall be regulated in such a manner that the residual field phase error shall be less than or equal to 0.2°.

## CHAPTER III. THE CLASSICAL CONTROLLER

Figure 1 of the introduction depicts in block diagram form the fundamental components of the previous electric field controller [7,8]. The amplifier chain consists of the items in the forward path of the control loop. Both of the compensators serve dual functions, i.e., summing junctions as well as lead-lag compensation. The procedure for analysis and design was to regard the accelerator as the dominant pole and all other devices as having poles further to the left in the left-half LaPlace transform plane (LHP). By placing one zero to cancel the accelerator pole, the bandwidth of the system was to be increased. However, this did not occur for reasons that shall now be described.

To begin with, let us describe in more detail the entire control loop system. The fundamental frequency of the accelerator is 1.3 Ghz. Due to heating and availability of high average power devices, the rf driver, klystron, and accelerator are operated in a pulse mode at a low duty cycle. For the LANL FEL the duty cycle is a 1 Hz pulse repetition rate and, typically, a 100 $\mu$sec macropulse pulse width. The macropulse is the collection of electron bunch micropulses, spaced every 46.2 nsec (the inverse of 21.67 Mhz) (Fig. 8). The amplifier chain from the oscillator to the rf driver is continuous wave (CW). As a result, the compensators must

compare a pulse signal to a CW signal in order to determine the field error.

The reference signals are both empirically determined. The amplitude is set by invoking a field level monitor or more often by injecting electrons into the accelerator and measuring their energy. Likewise, the manual phase shifter #1 is adjusted until the macropulse of electrons have minimum energy spread and/or maximum current transport through the structure (Fig. 1).

The electronically variable phase shifter and attenuator are shown in more detail in Fig. 9. The phase shifter is basically a three port circulator with one port terminated with metal-oxide semiconductor (MOS) diodes. The circulator accepts power in one port and transmits the signal unaltered to the adjacent port. If the power flow from the first port to the third port were interrupted by a device which changes only its capacitance, the resulting effect would be equal to a line length change. Therefore, an incident rf signal into port one will be endowed with a phase shift when it exits port two and travels to port three. The variable attenuator uses p-i-n diodes that vary their current conduction under the influence of a varying bias signal. Both of these devices are designed to mitigate their inherently high rf power reflection coefficients. This will allow each of them to operate autonomously from one another.

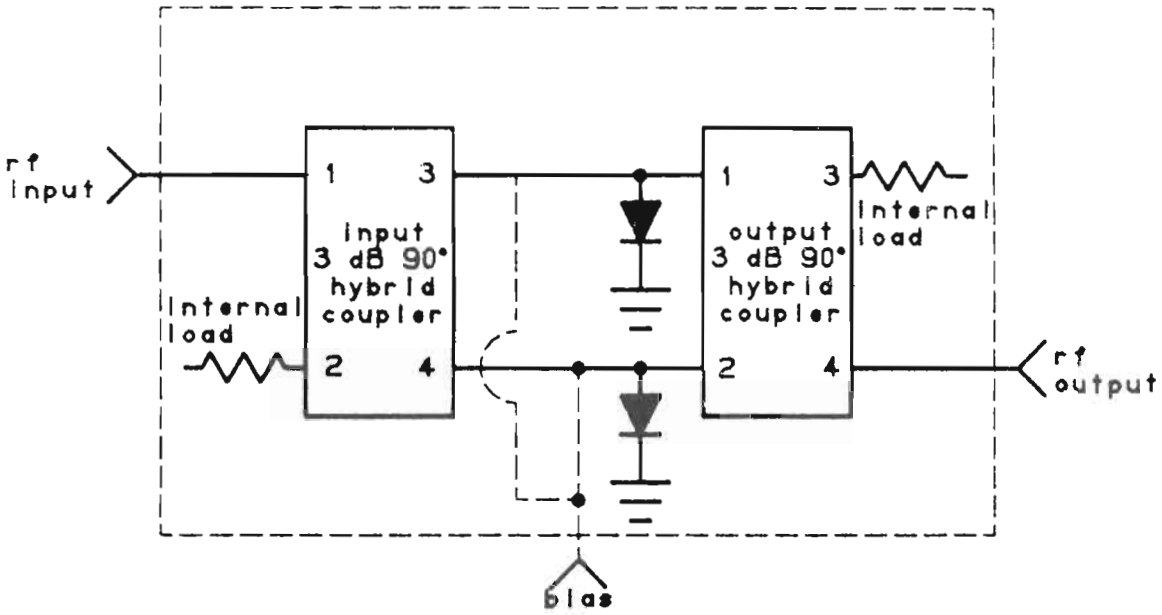


a) electronically variable attenuator

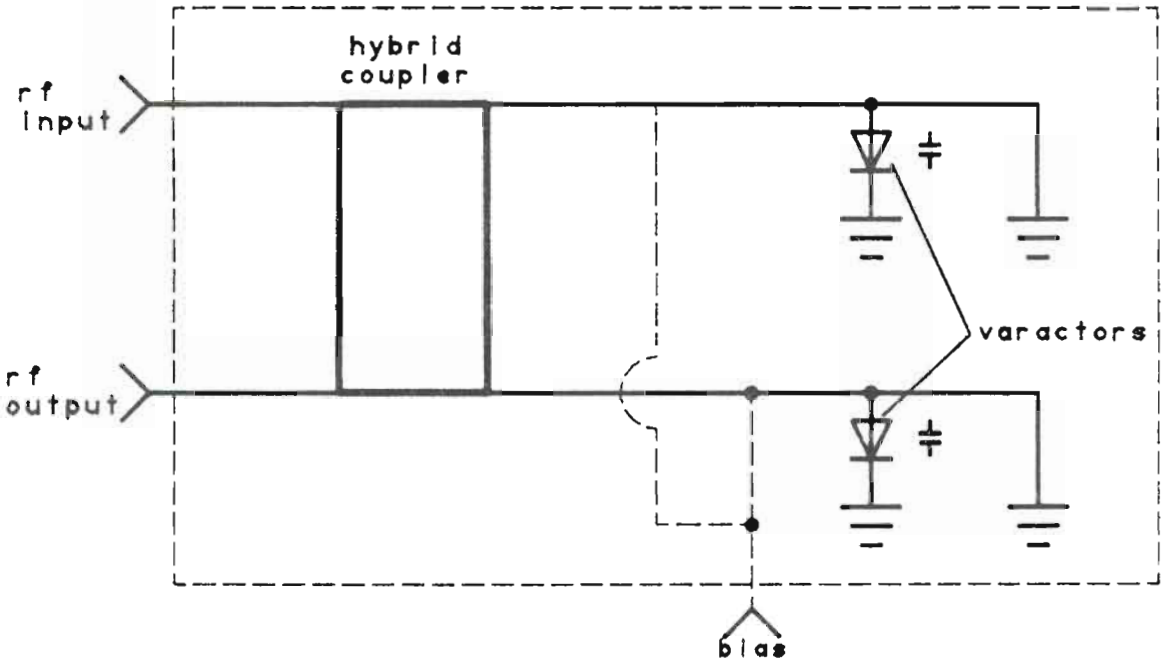


b) electronically variable phase shifter

FIGURE 9 Phase and Amplitude Modulators.

Both devices modulate the input signal to the rf driver in order to reduce amplitude and phase errors to zero. Since the phase and the amplitude of any signal are intricately related, the phase modulator must have its input power at a saturated level. This is to guarantee no amplitude change for any given phase change. The problem is that the device is now nonlinear. In order to achieve an adequate linear phase range, the device must have its saturated input level reduced. Hence, in practice there is a limit to its guaranteed amplitude invariance. Similarly, the variable attenuator will have a phase shift for a given amplitude change. But in the attenuators case, the amplitude obviously can not be saturated. One way to circumvent this phase problem is to design the amplitude modulator to have at least a decade more bandwidth than the closed-loop control system's bandwidth. In this way, the phase shift over the frequency interval of interest will be minimized. P-i-n diodes are inherently nonlinear and, in order to achieve linearity, the diodes must be operated high up on their current-voltage curve. The effect is to unnecessarily attenuate rf power, which, in turn, requires re-amplification. The overall result is that controller-produced phase modulations produce small amplitude variations, and visa versa.

Because reliable components (such as operational amplifiers) do not have appreciable gain at 1.3 Ghz, and with the goal of regulating the amplitude as well as the phase of

the accelerator fields, the output signal was resolved into its constituent components. The output feedback signal was rectified and low-pass filtered in order to obtain its amplitude level. A double-balance mixer (DBM) was used as a phase detector. The DBM's principal of operation is that when two identical frequency signals of equal power are incident onto the two input ports, the output port will have the sum and difference frequencies. With the sum frequency low-pass filtered, the remaining difference signal will be zero hertz. This DC output will then have variations in it that directly correspond to the phase difference between the two input signals.

Neither of the detectors are linear nor wideband for a large class of input signals. The DBM is linear only over a phase range of ±30°. This is easily seen when you consider that the two input rf signals are sinusoidal. For a large input phase difference, the output will have a sinusoidal shape. As discussed earlier, the rectifying diode will only be linear for a large input signal, and nonlinear for a small input signal [9]. This is seen by studying the simple diode equation, which is given by

$$I_D = I_{SAT} \left(e^{-qV/kT}-1\right) \quad . \tag{10}$$

Both control loops are unity feedback with the compensators in series with the plant. They both have the same form, i.e., lead-lag filters. One pole and one zero, which are experimentally tuned and determined. Equation 11 gives the structure of the filter;

$$C(s) = \frac{K(s+b)}{s+a} \quad . \tag{11}$$

Using a Hewlett-Packard audio network analyzer, the tuning range of the compensation was determined to be from

$$C_1(s) = \frac{79x10^6}{(s+ 18.85x10^3)} \tag{12}$$

to

$$C_2(s) = \frac{70(s+ 1131x10^3)}{(s+ 18.85x10^3)} \quad . \tag{13}$$

The two ranges of compensation were derived from actual Bode diagrams produced by the analyzer. (NOTE: This data is for the entire compensator board, from input to output.)

If the plant for the phase circuit (phase modulator, amplitude modulator, rf driver, klystron, and accelerator) is linearized, then it will have an input-to-output nominal transfer function given by equation 14;

$$G_o(s) = \frac{3.2x10^{12}}{(s+1.1)(s+7.9)(s+40.9)(s+7.3)(s+12.4)} \quad . \quad (14)$$

Therefore, the loop gain function is given by

$$G_o(s)\,C(s)\,H_o(s) = \frac{3.20x10^{12}}{(s+1.1)(s+7.9)(s+40.9)(s+7.3)(s+12.4)} \cdot$$

$$\frac{K(s+1.1)}{(s+0.02)} \cdot \frac{0.16}{1.7x10^{8}} \quad , \quad (15)$$

where C(s) is the compensator given previously, and $H_o(s)$ is the feedback signal's attenuation. The linearized amplitude circuit (amplitude modulator, rf driver, klystron, and accelerator) has its nominal transfer function shown in equation 16,

$$G_o(s) = \frac{3.2x10^{10}}{(s+1.1)(s+7.9)(s+40.9)(s+7.3)} \quad , \quad (16)$$

and its corresponding loop gain function is given by

$$G_o(s)\,C(s)\,H_o(s) = \frac{3.2x10^{10}}{(s+1.1)(s+7.9)(s+40.9)(s+7.3)} \cdot$$

$$\frac{K(s+1.1)}{(s+0.02)} \cdot \frac{1}{1.7x10^{8}} \quad . \quad (17)$$

(NOTE: Equations 14 through 17 were scaled by a factor of $10^6$.)

As can be seen from the two equations the two control loops have different dynamics, i.e., the phase loop has one more dynamic element. Because a pole is contributed by the compensator that is close to the origin, good phase and gain margins could not be achieved. In fact, in actual practice unacceptably small margins were the norm. This is because the control system design was oversimplified, and the resulting compensator was too simple. In order to achieve good performance the stability requirement was relaxed and the feedback gains were maximized until the loops oscillated, then slightly reduced in order to achieve a small measure of stability. Therefore, this performance versus stability philosophy resulted in the designed margins being reduced to near zero.

The loop gain function descriptions would be more complete if the transfer function of the detectors were included. But without writing them as nonlinear functions, the resulting system equation would be virtually useless.

Both loops, therefore, are very nonlinear, rendering accurate analysis very difficult if not impossible. The closed-loop gain using this compensation scheme was 2 and the unity gain bandwidth was ≈200 Khz. The residual field errors were 1% for the amplitude and 1° for the phase. However, even with these problems, the experimenters were able to achieve

sufficient control of the electric fields for optical wavelength and intensity stability of the FEL. This is due to several reasons: 1) the controllers were tuned several times during the course of an experiment, 2) accelerator parameters were kept as near constant as possible, and 3) the experimenters were able to discern useful information even though the FEL performance was poor due to rf instabilities. In general, the stability and performance of the rf fields will never be good enough because the FEL will always demand better control [10]. As an example, frequency sideband growth can now be observed during particular FEL operating modes. Present methods developed to deal with this problem involve interaction with the optical beam, hence are subject to eventual failure. One theory postulates that the growth mechanism can be subdued if the rf instabilities were reduced. However, to date, nobody has been able to achieve these demanding control fluctuation levels, hence, the theory has never been validated. The next chapter describes a method that is a step in that direction.

# CHAPTER IV. THE MODERN CONTROLLER

## A. Analysis and Design

The primary deficiency with the previous controller was with its design philosophy and hardware implementation. Therefore, the new design philosophy is to include all of the necessary dynamics. This and the use of more linear components will achieve better control. Three objectives were decided upon as a measure of success: 1) constant controller tuning reduced, 2) phase and amplitude fluctuations reduced, and ultimately 3) the FEL optical performance increased. To meet these objectives the entire previous controller scheme was discarded, leaving only the oscillator, the rf driver, the klystron, the accelerator, and their support equipment.

There are various methods available to the control engineer, but the method selected by the author was an optimal linear quadratic regulator (LQR) state-feedback [11]. It held the promise of excellent stability robustness margins; namely, infinite forward gain margin, 50% gain reduction margin, and at least ±60° phase margin (Fig. 10). These optimal LQR properties have no real engineering significance, but since stability does, they play a key role in the design process. The measurements of the plant parameters can easily have errors as large as 25%, and; therefore, necessitates the optimal LQR stability properties.

An additional part of the new design philosophy is to keep things as simple as possible, but no simpler. The approach attempted here was then to model the system by its first-order approximation. This would then make the model computationally as well as theoretically very tractable and also allow easier understanding of the actual physical control process. In keeping with this philosophy, all dynamic elements were modeled as first-order loss-pass equivalent filters. The low-pass equivalency retains generality because the control system bandwidth arises from the low-pass demodulated version of each signal. The rf driver and the accelerator have normal, smooth low-pass equivalent frequency transfer functions. However the klystron does not. Its gain-frequency curve is asymmetric. Below the center frequency, the gain rolloff rate is less than it is above the center frequency. For frequencies close to the center (1.3 Ghz $\pm$ 4 Mhz) the gain curve is flat. Because the open-loop system is stable, off-line identification was performed, and the uncertainty in the nominal plant model was reduced.

Before proceeding to the derivation of the model, an understanding concerning the selection of the states is necessary. Experimental selection of a state follows from its basic definition.

> Definition 3: The state of a dynamic system is the smallest set of physical variables such that the

knowledge of these variables, together with the input, completely determine the system's behavior [12].

Since we wish to control the electric fields in the accelerator, which are produced by the rf power flowing into the accelerator, the minimum set is formed by the output of each of the amplifiers and the accelerator. The measure of the electric field inside the accelerator is technically an output variable and not a state. Its value is precisely what we are trying to control by using the states and the input. However, by considering this output signal to be a constant times the field, one can realize a three, instead of a two, state system model. This three state model will now have the advantage of controlling the output as well as the states of the system. Including internal amplifier physical variables would be more than sufficient and hence would form a nonminimal set. These states, together with the input, then precisely determine the complete behavior of the system.

As discussed earlier, the primary tool for modeling will be Bode frequency analysis from input to output of each subsystem's low-pass demodulated signal. The rf driver was measured to have a -3db frequency point of 1.26 Mhz and a power gain of 40 db. Therefore, using the low-pass filter form, which is given by

$$A(s) = \frac{K}{\tau s+1} \quad , \tag{18}$$

where K = the D.C. gain

$\tau$ = the amplifier time constant (inverse of -3db frequency point; in rad/sec)

we have

$$A(s) = \frac{7.9\times10^{10}}{(s+7.9\times10^{6})} \quad . \tag{19}$$

Likewise, the klystron has its description approximated by

$$B(s) = \frac{4.1\times10^{11}}{(s+40.8\times10^{6})} \quad . \tag{20}$$

Before stating the model of the accelerator, let us first describe its equivalent circuit (Fig. 11). A cavity can be modeled as a series circuit composed of an inductor L, capacitor C, and a series resistance $R_s$. The measurable quantities $\omega_o$, center frequency, $Q_o$, unloaded quality factor, and $R_o$, shunt impedance (previously defined) are necessary and sufficient for the description of a resonant cavity operating in a particular mode. If $\omega_o$, $Q_o$, and $R_o$ are measured, they are related to the equivalent circuit parameters by

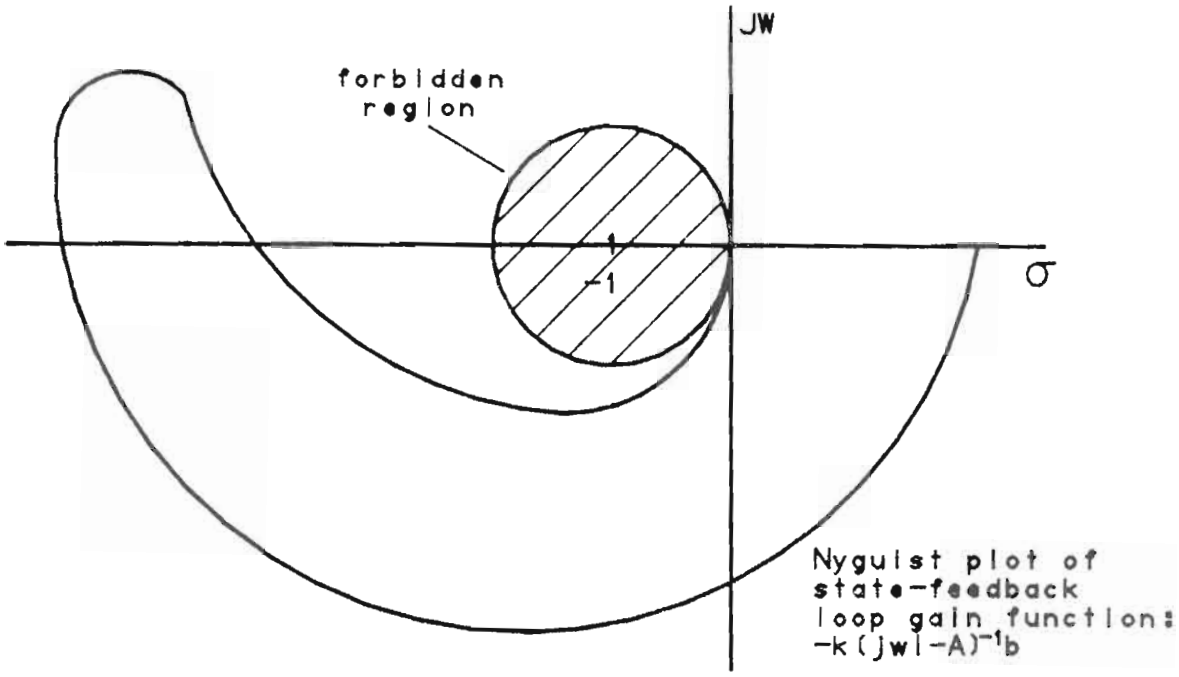


FIGURE 10 Optimality Condition.

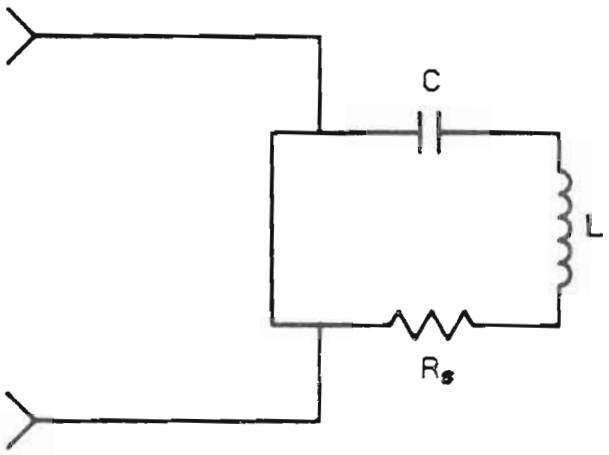


FIGURE 11 Equivalent Circuit of Resonant Cavity.

$$L = \frac{R_o}{\omega_o Q_o} \quad , \tag{21}$$

$$C = \frac{Q_o}{\omega_o R_o} \quad , \tag{22}$$

$$R_s = \frac{R_o}{Q_o^2} \quad . \tag{23}$$

Qualitatively, $R_o$ is a measure of the on-axis electric field available for acceleration compared to the power needed to overcome any losses and establish this field (Fig. 6). The cavity's time constant is given by

$$\tau = \frac{Q_o}{\omega_o(1+\beta)} \quad , \tag{24}$$

where $\beta$ = the coupling coefficient.

The coupling coefficient $\beta$ describes the ratio of the coupled generator impedance to the cavity impedance. For the control experiment, the accelerator used had a $Q_o$ = 18,465 and a $\beta$ = 1.4. Therefore, the cavity's time constant is 0.94 $\mu$sec, and using the low-pass filter equation;

$$C(s) = \frac{K}{\tau s+1} \quad , \tag{25}$$

we have the accelerator's low-pass demodulated equivalent transfer function;

$$C(s) = \frac{9.5x10^5}{s+1.1x10^6} \quad . \tag{26}$$

To account for some loses between the klystron and the accelerator, a K = 0.95 was chosen. The convolution of all three transfer function, A(s), B(s), and C(s), form the system plant transfer function, or

$$G(s) = \frac{(7.9x10^{10})(4.1x10^{11})(9.5x10^5)}{(s+7.9x10^6)(s+40.8x10^6)(s+1.1x10^6)} \quad . \tag{27}$$

Dividing G(s) by $10^6$, we now have the scaled system function

$$G(s) = \frac{3.1x10^{10}}{(s+1.1)(s+40.8)(s+7.9)} \quad . \tag{28}$$

Converting the transfer function G(s) to one of the canonical state space forms gives

$$dx/dt = (A_0+\delta A)\ x + (b_0+\delta b)\ u \tag{29}$$

$$y = Cx \quad , \tag{30}$$

or

$$dx/dt = \begin{bmatrix} -1.1 & 1 & 0 \\ 0 & -40.8 & 1 \\ 0 & 0 & -7.9 \end{bmatrix} x + \begin{bmatrix} 0 \\ 0 \\ 3.1x10^{10} \end{bmatrix} u \qquad (31)$$

$$y = [1\ 0\ 0]\ x \qquad (32)$$

where x = the vector of states (Fig. 2)

u = the scalar input

y = the scalar output.

The transfer functions and state space descriptions each have uncertainty in their time constants and DC gain. The uncertainty enters the state space equations as

$$\delta A = \begin{bmatrix} \pm 0.14 & 0 & 0 \\ 0 & \pm 3.1 & 0 \\ 0 & 0 & \pm 0.5 \end{bmatrix} , \qquad (33)$$

and

$$\delta b = \begin{bmatrix} 0 \\ 0 \\ \pm 1.2x10^{10} \end{bmatrix} . \qquad (34)$$

Both the system transfer function and the state space description are for the nominal plant plus some additive uncertainty. It does not describe beam-loaded induced disturbances. These disturbances are characterized as both additive and multiplicative uncertainty. Inside the accelerator, the electron beam possesses two properties, a voltage and a current. Using Ohm's Law, the beam has an associated resistance. By making a series to parallel circuit transformation, the beam's impedance is in parallel with the cavity's shunt impedance. Since

$$Q_o = \frac{R_o}{\sqrt{\frac{L}{C}}} \quad , \tag{35}$$

the unloaded quality factor of the cavity will in fact be reduced, commensurately the cavity time constant will be decreased. The problem is that the current of the electron beam varies. Beam current can be defined as

$$I = \frac{q}{\Delta t} \quad , \tag{36}$$

where q = the total charge in micropulse

$\Delta$t = the micropulse pulse width.

If either q or $\Delta t$ change, the left-half plane pole contributed by the accelerator will also change. Typically, the total charge from the electron injector will be at its greatest value at the beginning of an experiment, but towards the end, the total charge will be smaller. The result is a slowly migrating pole towards the rith-half plane.

The electron beam removes energy from the electric fields; therefore, they are lower in value and incorrect for succeeding electron bunches. The electron bunches perturb the fields at a frequency of 21.67 Mhz. This is beyond the limits of the rf control system's bandwidth (the reasons were discussed in Chapter I). However, if during the electron macropulse, the current is relatively constant, a steady-state condition will be reached. That is, the electron beam energy removal rate will equal the rf control system's field restoration rate. The time constant for this transient is identically equal to accelerator's time constant. The effect of this energy removal is an additive disturbance with a step function description and an instantaneous pole shift that is best described as multiplicative in nature. It is highly improbable, that the total charge changes greatly from one micropulse to another in a macropulse. However, from the beginning of an experiment to its conclusion, the total charge does change; in some cases as much as a factor of 5. The end effect is that the control system becomes less stable during the course of an experiment. This had dire consequences on

the previous output feedback controller technique. While sacrificing stability margin, the controller's loop gain was maximized for performance at the beginning of the experiment. As a result, towards the end of the accelerator experiment it would begin to oscillate very badly.

## B. Experimental Results

A Linear Quadratic Regulator (LQR) optimal control approach was used with the following choices

$$Q = \begin{bmatrix} 1 & 0 & 0 \\ 0 & 0 & 0 \\ 0 & 0 & 0 \end{bmatrix} \text{ and } r = 5x10^{10} \quad , \tag{37}$$

and the performance index was

$$J = \frac{1}{2}\int_0^\infty (x^T Q x + u^T r u)\ dt \quad . \tag{38}$$

Figures 12 through 18 show these results with and without beamloading. For phase measurement figures, the vertical axis is phase and the horizontal axis is time. The calibration factor is: 1 vertical division equals 2°. For amplitude measurement figures, the vertical axis is amplitude and the horizontal axis is time.

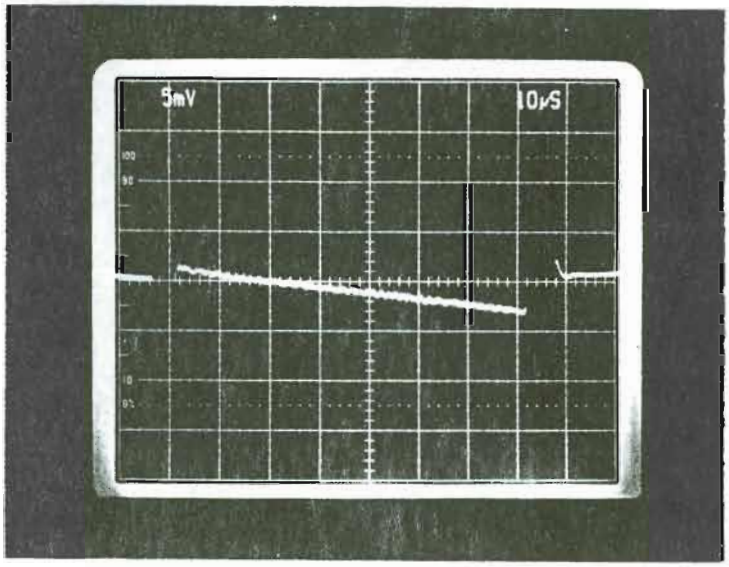


FIGURE 12 Closed-loop Optimal Regulator Phase Measurement without Beamloading Disturbance.

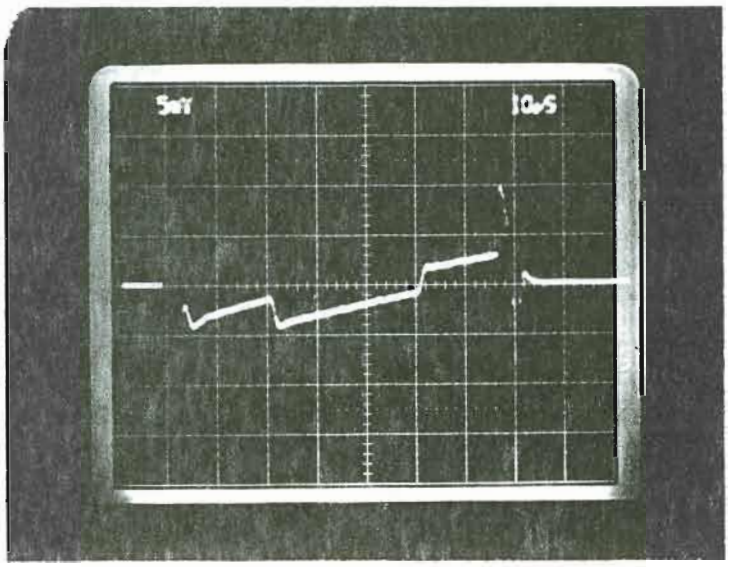


FIGURE 13 Closed-loop Optimal Regulator Phase Measurement with Beamloading Disturbance.

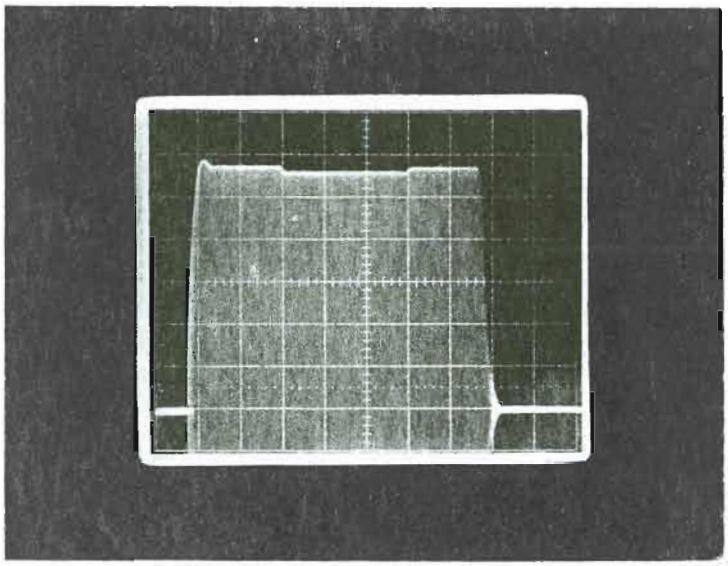

FIGURE 14 Closed-loop Optimal Regulator Amplitude Measurement with Beamloading Disturbance (50 mV/div and 10 μsec/div).

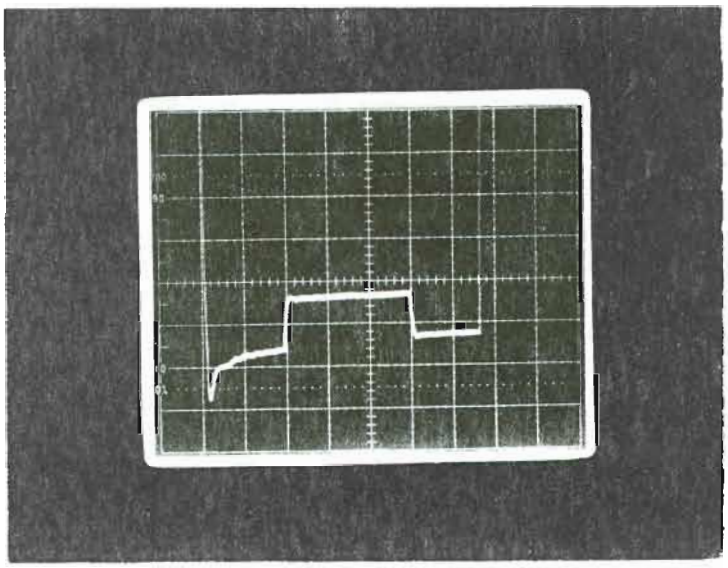

FIGURE 15 Expanded View of Closed-loop Optimal Amplitude with Beamloading Disturbance (5 mV/div and 10 μsec/div).

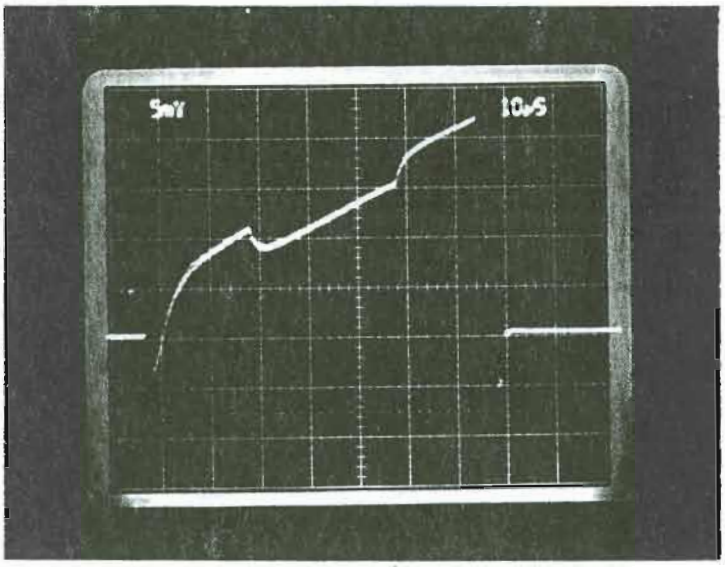


FIGURE 16 Open-loop Phase Measurement with Beamloading Disturbance.

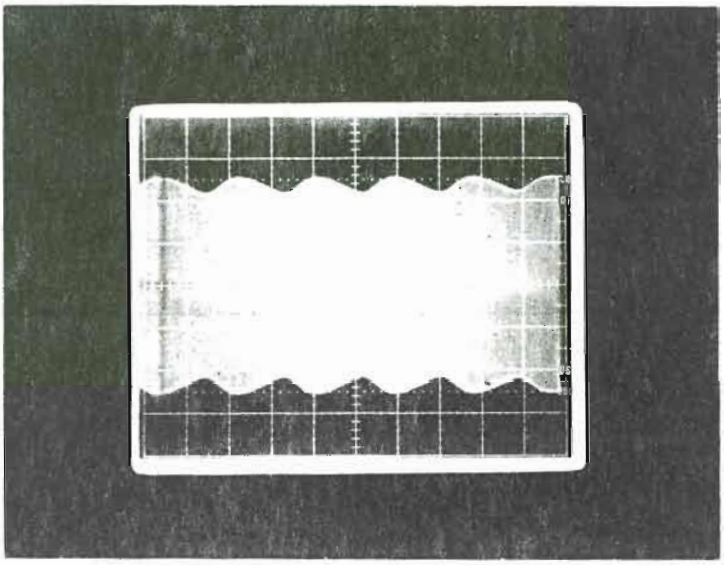

FIGURE 17 Unity Gain Bandwidth Measurement of Optinal Regulator (50 mV/div and 1 μsec/div).

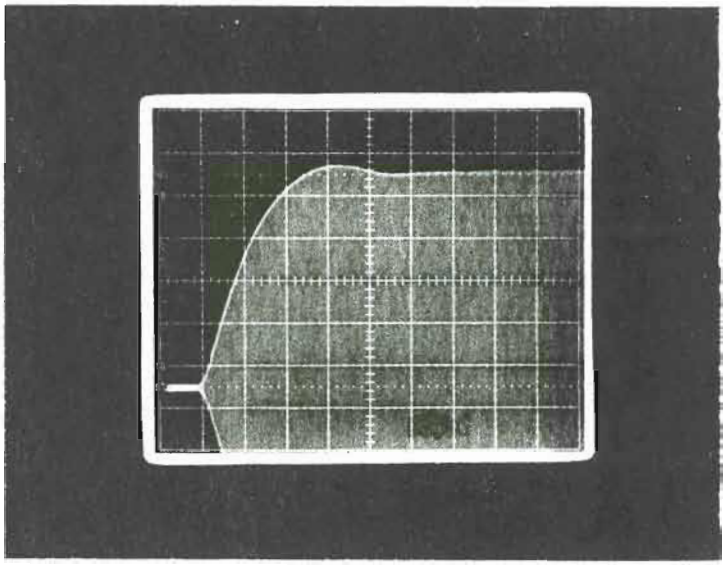

FIGURE 18 Closed-loop Optimal Regulator
Amplitude Risetime Measurement (1 $\mu$sec/div).

The phase margin was measured to be 41.5°. This measurement was performed, while the loop was closed, by changing the manual phase shifter #2 (Fig. 2) until the loop oscillated. Although one of the amplifiers failed during one control experiment, resulting in only one fourth the normal plant forward gain, the control system maintained its stability due to its inherent robustness.

As a result of this failure, the control loop was also brought into a soft nonlinearity. The klystron possesses a sector nonlinearity (normal operation of the accelerator precludes using this region). When the sector slopes were bounded by

$$\frac{1}{2} \leq \frac{P_{out}}{P_{in}} \leq \infty \quad , \tag{39}$$

and the reference input power increased (it was not known that the amplifier had failed), the state-feedback system was operated under optimal control conditions. Figure 19 shows this result.

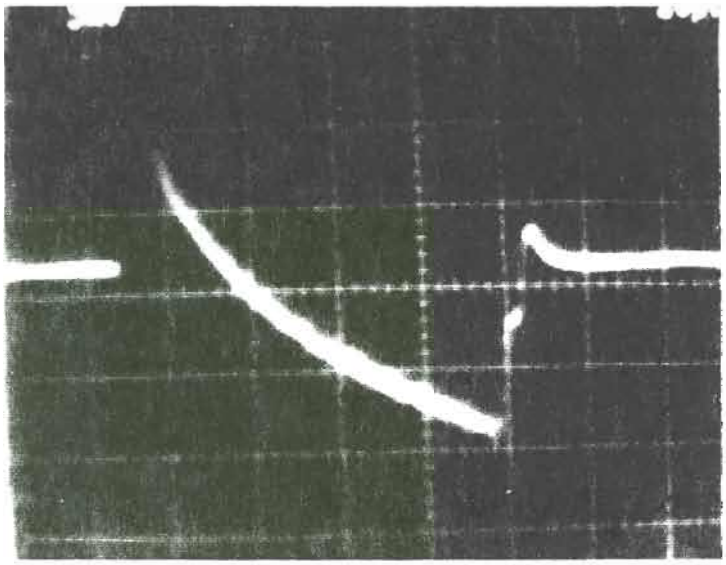

FIGURE 19 Closed-loop Optimal Regulator Phase Measurement with Nonlinear Operating Conditions and No Beamloading Disturbance (5mV/div and 10 μs/div).

The closed-loop optimal system was also operated under a much stronger nonlinearity, resulting in large oscillations.

In addition, different Q and r's resulted in different nominal performances, but the Q and r used in Figs. 12 through 19 had the best nominal performance and stability robustness.

The infinite gain margin of an ideal LQR design is destroyed by the fact that every loop has some finite time delay associated with it. This quantity is virtually impossible to measure in a physical system. The reason is that increasing the gain increases the loop bandwidth with the affect that time delay is no longer negligible. Gain margin measurements require that the phase remain constant but in physical systems this is never the case. Most often simultaneous perturbations occur in both the phase and gain of a system. In addition, extreme gain measurements could also involve nonlinearities due to saturation. Therefore, when the gain is increased, time delay becomes significant, phase shifts occur, nonlinearities become important, and all of these effects add together in some manner to cause instability. An easier task is to measure the gain reduction and phase margin. This is because phase shifting elements can be made out of near-ideal, lossless, transmission line, and gain reduction does not increase loop bandwidth, which would increase the importance of time delay, nonlinearities, etc.

Implementation of this rf state-feedback control system took only 3 hours versus 240 hours for the old technique. Also, feedback system implementation costs have been reduced by a factor of 11. The three phase shifters in the feedback

loops are used to negate the various line lengths at 1.2 GHz (Fig. 2). The gains are actually fixed microwave attenuators. The manual phase shifter #2 is used in order to ensure negative feedback. The summer is a passive, 180°, hybrid combiner. The manual phase shifter #1 and variable attenuator are used to experimentally set the correct reference input.

The residual accelerator field fluctuations are now less than 0.2%. Similarly, the phase fluctuations are less than 0.2°. This is in contrast to the 1.0% and 1.0°, amplitude and phase variations, respectively, which resulted from the output-feedback controller. The amplitude risetime is 1.6 μsec, for the LQR controller versus 4 μsec for output-feedback controller (Fig. 18).

## CONCLUSIONS

To date, the new control system has been operating continuously since October 11, 1989. With the exception of conducting control theory research, the controller has not had any need to be adjusted since that time. The original goals have all been met or exceeded, i.e., continuous tuning has ceased; loop gain has increased; the response has faster rise time with less overshoot; robustness against both known and unknown modeling errors and induced plant parameter variations has been achieved; passive, invariant components have been implemented; and the controller cost has been reduced.

Further research goals will be to include second-order variations and time-delay. On-line indentification shall be performed in order to determine a more accurate rf system model. Using this more accurate plant model, various control theories (e.g., $H\infty$ optimal control with a state-space realization, frequency-shaped robust optimal control, proportional plus integral state-feedback, etc.) will be investigated, and based upon these results, a "best" controller will be selected and implemented. In addition, simultaneous accelerator control using only one rf system will be researched.

## BIBLIOGRAPHY


[1] W. E. Stein, W. J. D. Johnson, J. F. Power, and T. J. Russell, "Stability Requirements of RF LINAC-Driven Free-Electron Lasers," 11th Int. FEL Conf., Naples, FL, Aug. 29-Sept. 1, 1989, to be published.

[2] Stanley Humphries, Jr., Principles of Charged Particle Acceleration, John Wiley and Sons, 1986.

[3] B. C. Knapp, E. A. Knapp, G. J. Lucas, and J. M. Potter, IEEE Trans. Nucl. Sci., NS-12, p. 159, 1965.

[4] Any IEEE Trans. Nucl. Sci.

[5] Amnon Yariv, Quantum Electronics, John Wiley and Sons, 1989.

[6] Thomas Marshall, Free-Electron Lasers, MacMillian Pub. Co., 1985.

[7] R. Jameson, "Analysis of a Proton Linear Accelerator RF System and Application to RF Phase Control," Los Alamos Nat. Lab., Los Alamos, NM, Rep. LA-3372, Nov. 1965.

[8] Michael T. Lynch, private communication.

[9] S. M. Sze, Physics of Semiconductor Devices, John Wiley and Sons, 1981.

[10] Roger W. Warren, private communication.

[11] B. D. O. Anderson and J. B. Moore, Optimal Control: Linear Quadratic Methods, Prentice-Hall, Inc., 1990.

[12] K. Ogata, Modern Control Engineering, Prentice-Hall, Inc., 1970.

[13] M. J. Grimble and T. J. Owens, "On Improving the Robustness of LQ Regulators," IEEE Trans. Auto. Control, AC-31, p. 54, 1986.

[14] R. E. Kalman, "When Is a Linear Control System Optimal?," Trans. ASME Ser. D: J. Basic Eng., Vol. 86, p. 1, 1964.

[15] W. E. Hopkins, Jr., "Optimal Control of Linear Systems with Parameter Uncertainty," IEEE Trans. Auto. Control, AC-31, p. 72, 1986.

[16] J. D. Cobb, "Linear Compensator Designs Based Exclusively on Input-Output Information are Never Robust with Respect to Unmodeled Dynamics," IEEE Trans. Auto. Control, Vol. 33, p. 559, 1988.

[17] A. Tesi and A. Vicino, "Robust Stability of State-Space Models with Structured Uncertainties," IEEE Trans. Auto. Control, Vol. 35, p. 191, 1990.

[18] A. K. El-Sakkary, "A New Criterion for Estimating Robust Time Delays for Closed-Loop Stability," IEEE Trans. Auto. Control, Vol. 35, p. 209, 1990.

[19] I. R. Peterson, "Complete Results for a Class of State Feedback Disturbance Attenuation Problem," IEEE Trans. Auto Control, Vol. 35, p. 1196, 1989.

[20] B. R. Barmish and Z. Shi, "Robust Stability of Perturbed Systems with Time Delays," Automatica, Vol. 25, p. 371, 1989.